Updated contribution “Advances in Fluid-Structure Interaction” from the ERCOFTAC Symposium on Unsteady Separation in Fluid-Structure Interaction, June 17-21, 2013, Mykonos, Greece

TURBULENCE NEAR INTERFACES – MODELLING AND SIMULATIONS

J. C. R. HUNT[1], T. ISHIHARA[2], D. SZUBERT[3], I. ASPROULIAS[3], Y. HOARAU[4], M. BRAZA[3]

[1] Department of Earth Sciences, University College London, London WC1E 6BT, UK
[2] Department of Engineering, Nagoya University, Nagoya, Japan
[3] Institute of Fluid Mechanics of Toulouse, UMR CNRS 5502, 31400 Toulouse, France
[4] ICUBE UMR CNRS 7357, 67000 Strasbourg, France

julian.hunt@ucl.ac.uk, ishihara@cse.nagoya-u.ac.jp, Damien.szubert@imft.fr, ioannis.asproulias@imft.fr, hoarau@unistra.fr, marianna.braza@imft.fr

We consider well-developed inhomogeneous turbulent shear flows in the *x* direction that are bounded by interfaces (*I*) separating regions of turbulent and non-turbulent (or weak turbulent) flows. The interfaces are approximately continuous and there is no large-scale forcing (by body forces or external turbulence) in these flows, see fig 1. The mean velocity is $\bar{u}$ with significant mean shear $S=\nabla\bar{u}\sim\Delta U_o/L$, which is comparable with the large scale strain in the turbulence, $\Sigma\sim u_o/L$, where u_o is the *rms* turbulence, which is of the order of the large scale velocity fluctuations , i.e. $\Delta U_o\sim u_o$.

The fluctuating interface location y_I at given *x*, *z* and given time is defined by where the normal gradients of fluctuating vorticity are maximum (Bisset et al 2002). In all types (without forcing or external straining flow) there is a significant mean ‘boundary entrainment velocity’ $E_b=dy_I/dt$ which is of order u_o. As Prandtl originally suggested, (see Bodenschatz & Eckert 2011), the *rms* fluctuations of E_b, E_b', relative to its mean value $\overline{E_b}$ are related to the structure of the interface and the whole flow. There may or may not be a significant mean normal velocity, the ‘entrainment velocity E_v’, which can be comparable with u_o, as found in jets.

The properties of the turbulence near the interface $y=y_I(x,z,t)$ on the edge of well developed shear flows has been the object of a number of recent studies, Ouvrard et al (2010), Westerweel et al (2009), Eames & Flor (2011), Hunt et al (2008, 2011), Braza et al (2010), Braza (2012), and can be summarised as follows.

(a) Thin shear layers form at the continuous interface between sheared turbulent flow ($y<y_I$) and the exterior region where there is weak turbulence with weak shear. There is a jump in the large-scale velocity, $\Delta U_{0,}$ (defined conditionally relative to the interface) with fluctuations of the order of u_o and a mean jump velocity $\langle\Delta U_I\rangle$. The mean thickness of these sheets

l_I is of the order of the Taylor micro scale (λ). Fig 2 shows the conditional profile for a turbulent boundary layer. There may be a jump in the scalar concentration of order ΔC_i .

(b) The locations y_I of the interfaces fluctuate (in a moving frame) on time scales of order L/u_o . The ratio *Ri* of the *rms* fluctuations of y_I , $y_I{}'$, to the integral length scale L of the turbulence in the shear flow depends on the type of shear flow. When *Ri* >~*l* the interface fluctuations are large and the shape of the interface is convoluted (i.e. y_I may have 2 or more values). Whereas when *Ri* <<1, the fluctuations are smaller and the interface is single valued. In the former case external fluid is directly transported or 'engulfed' into the internal fluid, while in the latter case there is small-scale eddy transport and molecular transport at the interface, i.e. 'nibbling' (Mathews & Basu 2002). For the same range of values of *Ri*, dominance of 'engulfing' or 'nibbling' there is a local form of the flow near the interface. It is found that the profile of the conditionally sampled velocity field relative to the interface i.e. $\overline{u}(\tilde{y})=\langle U\rangle$, where $\tilde{y}=y-y_I$, is similar near the outer edge of different shear flows (Westerweel et al 2009).

(c) The main features of the dynamics of the flow outside and within the interfacial layers are as follows.

(i) Growth mechanisms and conditional profiles are affected by the inflection points in the mean conditional profile $\langle\tilde{U}\rangle(\tilde{y})$. For jets, wakes and plumes these occur at the outside of the interface, i.e. $d^2\langle\tilde{U}\rangle(\tilde{y})/d\tilde{y}^2=0$, where $\tilde{y}=0$. For these types of shear layer the most energetic eddies are produced by the conditionally averaged shear $d\langle U\rangle/dy$ within the turbulent region (i.e. non-modal or `rapid distortion' or `horse shoe' eddies (Hunt & Carruthers 1990, Ferre et al 1990)). However in boundary layers and mixing layers the inflection point in $\langle\tilde{U}\rangle(\tilde{y})$ occurs in the interior of the shear flow, approximately where the interface shear layer joins the internal shear layer, i.e. at $\tilde{y}=-l$. Since the unstable normal modes of these profiles have a large magnitude within the turbulent region on the scale *L*, there are larger indentation of the interface $y_I{}'/L\sim 1$ and larger fluctuations in the boundary entrainment velocity i.e. $E_b{}'/E_b\sim 1$ and *Ri* ~1.

(ii) Within the thin interfacial shear layer, whose thickness ℓ is of order λ, as small scale vortical eddies are stretched by the shear, their typical radius reduces to the Kolmogorov microscale $l_v\sim L\cdot Re^{-3/4}$ (da Silva & dos Reis 2011).

(iii) The key external influence of the interfacial shear layers is that it 'blocks' the smaller scale eddies of the turbulent region (which move at the local mean velocity) and distorts their vorticity as they impact onto the layer (Hunt & Durbin 1999, Turfus & Hunt 1987). The blocking leads to a decorrelation of velocity fluctuations across the interface. (Ishihara et al 2015) Also these distortions lead to the sharp mean velocity gradients within and outside the layers (Hunt et al 2008). However the larger scale eddy motions inside the interface move at the average speed across the shear flow which differs from the local speed at the interface. They are not blocked but stimulate irrotational fluctuations in the exterior region (Carruthers & Hunt 1986; Bissett et al 2002), see fig3. The combined contribution of the small and large scales leads to a jump in the Reynolds stress across the layer from zero outside to $\Delta\tau$ just inside the interfacial layer.

(iv) As the vortex sheet of the interfacial shear layer moves in the *y*-direction with velocity E_b, there is a local acceleration (~ E_b $\langle \Delta U_I \rangle / l_I$), which is balanced by the gradient in the Reynolds stress in the layer ($\Delta\tau / l_I$). Integrating the *x*-component of the mean momentum equation across the layer shows how the mean product of the mean and fluctuating boundary entrainment velocity and the mean and fluctuating velocity jump $\langle \Delta U_I \rangle'$ momentum flux is balanced by the jump in shear stress, i.e.

$$\langle E_b \rangle \langle \Delta U_I \rangle \cdot (1 + Ce) = -\Delta\tau \quad .$$

The entrainment coefficient

$$Ce = \langle E_b{}' \cdot \langle \Delta U_I \rangle' \rangle / (\langle E_b \rangle \langle \Delta U_I \rangle)$$

is of order 1 when the engulfment is greater than 'nibbling' (as DNS of turbulent boundary layers demonstrate), and small when nibbling dominates (as with wakes and jets Westerweel et al 2009).

(d) The above studies enable an adaptation of the Organised Eddy Simulation, OES method (Braza et al 2006, Braza et al 2008, Bourguet et al 2008), to better capture interfacial layers at the same time as using economic grids. In the OES method the resolved velocity field $U(x,t)$ is the ensemble-average of the exact velocity representing all the coherent processed and the turbulent fluctuation $\hat{u}$ represents all the random turbulence processes. The second moments of this field are especially modelled by means of tensorial eddy-viscosity modelling that captures quite well the turbulence stress anisotropy. Thus

$$u^{¿} = U(x,t) + \{\hat{u}(x,t)\} \quad ,$$

where $\{\}$ denotes the component that is only defined statistically.

In the Improved OES method (**IOES**), an intermediate random velocity field V_{RI} is introduced, by means of the high-order POD (Proper Orthogonal Decomposition) modes (Szubert et al, 2015). The method first requires estimating the position of the continuous interface $y_I(x,t)$ from the OES field, using the dynamical criterion for the interface (e.g. max of dissipation or shear) and then computing its mean and fluctuating positions i.e. $\langle y_I(x,z,t) \rangle$ and $y_{I'}$. (e.g. as in Deri et al 2011).

In order to model the effects of the different types of eddies impacting on the interface, $y_I(x,t)$ is filtered into 'large' and 'medium' scales. The new step in the IOES method is to introduce at each time step a random explicit intermediate velocity field $\{\check{u}\}$. $\check{u}$ is calculated in terms of the OES velocity, i.e. $U(x,t)$ near the interface, using the theory of blocking by the interfacial layer for the medium to small scales and irrotational transformation for the large scales, as explained in (iii) above (see also Turfus & Hunt 1987). The sharp gradients associated with the intermediate velocity field also lead to a correction to the statistically modelled Reynolds stresses (i.e. for medium and small scales).

The dynamical effect of the interaction between of the intermediate field and the OES field together with the corrected statistical Reynolds stresses, were modelled by Hunt et al (2008), which showed how the interfacial layer remains sharp through the distortion of eddies near interface. The theoretical base of this model is achieved by considering higher-order POD (Proper Orthogonal Decomposition) modes for the stochastic forcing of the kinetic energy and dissipation transport equations (Braza, 2012). This is created by a randomly fluctuating forcing term in the dissipation rate of these equations (Braza et al 2013) containing a kinetic-energy scale reconstructed by higher-order POD modes, as presented in the following.

$$\frac{\mathrm{D}\varepsilon}{\mathrm{D}t} = \frac{\varepsilon}{k}\left(C_{\varepsilon 1}\, P - C_{\varepsilon 2}\, \varepsilon\right) + \frac{\partial}{\partial x_i}\left[\left(\nu + \frac{\nu_t}{\sigma_\varepsilon}\right)\frac{\partial \varepsilon}{\partial x_i}\right] + \frac{C_{\varepsilon 2}\, S^2_{\mathrm{POD}}}{k_{\mathrm{amb}}}$$

$$\frac{\mathrm{D}k}{\mathrm{D}t} = P - \varepsilon + \frac{\partial}{\partial x_i}\left[\left(\nu + \frac{\nu_t}{\sigma_k}\right)\frac{\partial k}{\partial x_i}\right] + S_{\mathrm{POD}}$$

$$S_{\mathrm{POD}} = \tilde{r}\, C_\mu\, \left(k^2_{\mathrm{amb}} + k^2_{\mathrm{POD}}\right)/\nu_{t\infty}$$

$$k_{\mathrm{POD}} = 0.5 \times \left(\overline{u^2} + \overline{v^2}\right)$$
$$k_{\mathrm{amb}} = k_{fs}\ U^2_\infty$$
$$k_{fs} = 3/2\ \mathrm{Tu}^2$$

This leads to a corrected value of $U(x,t)$.
It can be shown that the higher-order POD modes whose energy distribution is presented in Figure 4, precisely act within the shearing regions and in the separated areas, as well as between the shearing regions delimiting the wake, without 'contaminating' the irrotational regions. The present 're-injection' of turbulence in these regions characterised by the shearing mechanism and the Turbulent-Non-Turbulent (TNT) interfaces dynamics produces the "eddy-blocking effect" previously described and maintains these shear layers thin. This leads to a reduction of the wake's width and therefore to an improved drag force.
Figure 4 represents the transonic interaction around a supercritical airfoil, the OAT15A configuration, obtained by the present IOES approach. The interfacial shear-layer and the von Kármán eddies which span the whole shear layer are both quite well captured, as well as the buffet frequency of 78 Hz in good agreement with the experiments by Jacquin et al (2009). The results show in fig. 4 the sharper interfacial layer using the IOES method.
The present test-case has been one of the test-cases of the ATAAC (Advanced Turbulence Simulations for Aerodynamic Application Challenges) European program N° 233710, coordinated by DLR (D. Schwamborn), (March 2009 - June 2012). The method is also in application in the case of the so-called V2C supercritical laminar wing designed by Dassault Aviation, in the TFAST (Transition location effect on shock-boundary layer interaction) European project N° 265455 (2013-2016). Fig.5 shows the 3D buffet dynamics interacting with the shear layer and the von Kármán vortices of the near wake. Fig. 6 shows the energy of the three-dimensional POD modes as well as the signal and spectrum of the second POD temporal coefficient describing the buffet phenomenon and the spectrum of the 11-th order POD temporal

coefficient beyond which the influence of the von Kármán frequency bump becomes visible. Figure 7 shows the topology of the higher-order three-dimensional POD modes for the V2C configuration.

Acknowledgement
Part of this study has been carried out in the context of the European programmes ATAAC and TFAST. Part of the computing hours allocation has been provided by the French supercomputing centres CINES, IDRIS, CALMIP.

References

D. K. Bisset, J. C. R. Hunt & M. M. Rogers, (2002) "The turbulent/non-turbulent interface bounding a far wake", J. Fluid Mech., **451**, pp. 383-410.

E. Bodenschatz & M. Eckert (2011) Prandtl and the Gottingen school, in "A voyage through turbulence," Ed Davidson PA et al, Cambridge Univ Press

R. Bourguet, M. Braza, G. Harran & R. Elakoury, (2008) "Anisotropic Organised Eddy Simulation for the prediction of non-equilibrium turbulent flows around bodies", J. Fluids and Structures, **24** (8), 1240-1251.

M. Braza, J. Hunt, A. Jimenez-Garcia, D. Szubert, F. Grossi & Y. Hoarau, "Physical analysis of turbulent/non-turbulent interfaces in the transonic interaction around an airfoil by stochastic forcing and Organised Eddy Simulation", Key Note ERCOFTAC international Symposium "Unsteady Separation in Fluid-Structure interaction", Mykonos, Greece, June 17-21th, 2013.

M. Braza, "Turbulence modelling for strongly detached flows around bodies at high-Reynolds number, involving fluid-structure interaction", Key-Note Lecture, EMI/PMC Congress**,** Univ. Notre Dame, USA, 19 June 2012.

M. Braza, H. Ouvrard, R. Bourguet, R. Perrin (2010) "Turbulence modelling for strongly detached unsteady high-Re flows, based on refined PIV experiments", Key Note Lecture, CAIMS-SCMAI, Canadian Symposium on Fluid Dynamics (CSFD-2010),17-20 July 2010

M. Braza, R. Bourguet & R. El Akoury, (2008)"Organised Eddy Simulation for prediction of unsteady turbulent wake flows with thin interfaces", invited presentation, Mini-Symposium "Turbulent Interfaces", in "The European Consortium For Mathematics In Industry" - ECMI congress, London 30 June- 4 July 2008.

M. Braza, R. Perrin & Y. Hoarau, (2006) "Turbulence Properties in the cylinder wake at high Reynolds number", J. Fluids and Structures, **22**, pp. 757–771.

D.J. Carruthers & J.C.R. Hunt, (1986) "Velocity fluctuations near an interface between a turbulent region and a stably stratified layer", J. Fluid Mech. **165**, pp. 475-501.

C. B. da Silva & R. J. N. dos Reis, (2011) "The role of coherent vortices near the turbulent/ non-turbulent interface in a planar jet". Phil. Trans. R. Soc. A **369**, 738–753.

E. Deri, H. Ouvrard, M. Braza, J. Hunt, E.Cid & S. Cazin, (2011) "Capturing coherent structures and turbulent interfaces in wake flows by means of the Organised Eddy Simulation, OES and by Tomo-PIV", *Journal of Physics*, ***318***, *Conf. Series* 10.1088, paper presented in the 13th European Turbulence Conference, Sept. 2011.

I. Eames & J. B. Flor, (2011) “New developments in understanding interfacial processes in turbulent flows”, Phil. Trans. R. Soc. A, **369**, pp.702-705.

J. Ferre, J. C. Mumford, A. M. Savill & F. Giralt, (1990) “Three-dimensional large-eddy motions and fine-scale activity in a plane turbulent wake,” J. Fluid Mech. **210**, 371-414.

J. C. R. Hunt & D. J. Carruthers, (1990) “Rapid distortion theory and the problems of turbulence”. J. Fluid Mech. **212**, 497-532.

J.C.R. Hunt & P.A. Durbin, (1999) “Perturbed vortical layers and shear sheltering”, Fluid Dyn Res., **24**, pp.375-404.

J.C.R. Hunt, I. Eames, M. Braza, C. da Silva & J. Westerweel, (2011) “Interfaces in turbulence and implications for advanced modeling methods”, ERCOFTAC Bulletin, **87**, *invited.*

J.C.R. Hunt, I. Eames & J. Westerweel, (2008) “Vortical interactions with interfacial shear layers”, Proceedings of IUTAM conference on Computational Physics and new perspectives in turbulence, Nagoya, Sept 2006. Ed. Y. Kaneda. Springer Science, Berlin

J.C.R. Hunt, I. Eames, J.Westerweel, P.A. Davidson, S.Voropayev, J. Fernando & M. Braza “Thin shear layers – the key to turbulence structure?” Proceedings, Shallow Water Hydraulic Conference, Hong Kong, Dec. 2008.

T. Ishihara, H. Ogasawara & J. C. R. Hunt, (2015) “Analysis of conditional statistics obtained near the turbulent/non-turbulent interface of turbulent boundary layers,” J. Fluids and Structures, **53**, pp. 50-57.

L. Jacquin, P. Molton, S. Deck, B. Maury & D. Soulevant, (2009) “Experimental Study of Shock Oscillation over a Transonic Supercritical Profile”. AIAA Journal **47**(9), 1985-1994.

J. Mathew & A. J. Basu, (2002) “Some characteristics of entrainment at a cylindrical turbulence boundary”, Phys. Fluids **14** (7), 2065-2072.

H. Ouvrard, M. Braza, J. Hunt, G. Barbut & Y. Hoarau, (2010) “Capturing turbulent interfaces in wake flows by means of the OES approach”, invited presentation, EUROMECH Colloquium N° 517, “Interfaces and inhomogeneous turbulence”, 28 - 30 June 2010, UCL London.

D. Szubert, F. Grossi, A. Jimenez Garcia,Y. Hoarau, J. Hunt, M. Braza, “Shock-vortex shear-layer interaction in the transonic flow around a supercritical airfoil at high Reynolds number in buffet conditions”, J. Fluids & Structures, **55**, pp. 276–302, (2015).

C. Turfus, & J.C.R. Hunt, (1987) “A stochastic Analysis of the displacements of fluid elements in inhomogeneous turbulence using Kraichnan's method of random modes,” Advances in turbulence. 191-203.

J. Westerweel, C. Fukushima, J.H. Pedersen & J.C.R. Hunt, (2009) "Momentum and scalar transport at the turbulent/non-turbulent interface of a jet." J. Fluid Mech., **631**, pp. 199-230.

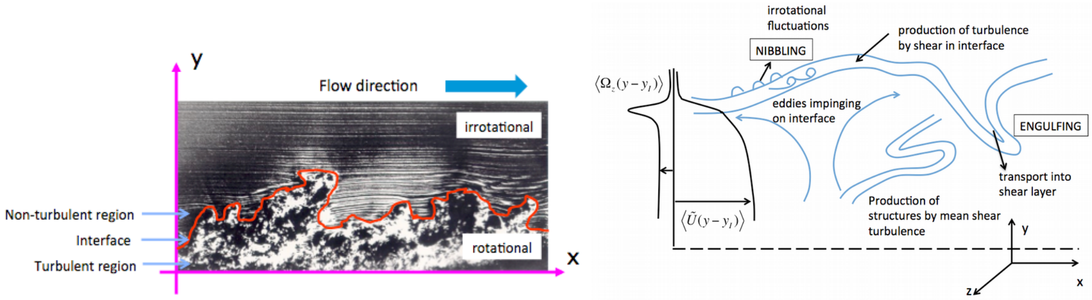

Fig. 1. A typical interface separating turbulence in shear layers from irrotational fluctuations outside. (a) High Reynolds number experiments of a turbulent boundary layer (from “Album of Fluid Motion” by Van Dyke). (b) Schematic diagram of the outer region of a wake or jet (when fully developed)

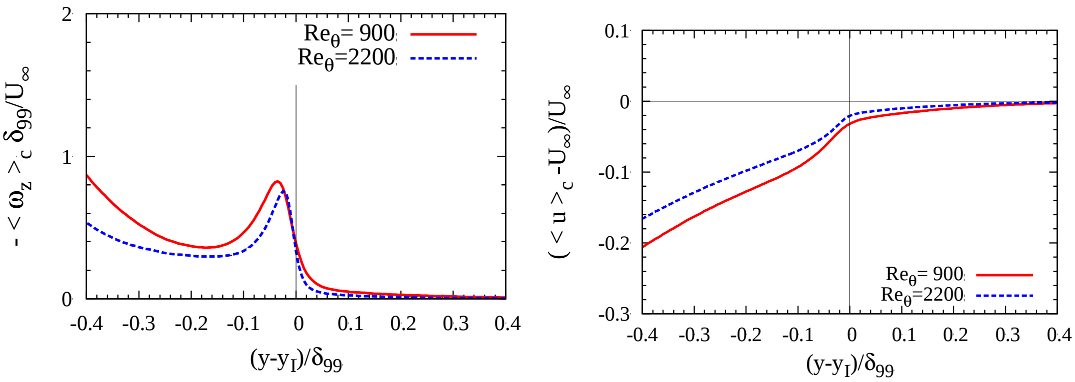

Fig. 2. Direct Numerical Simulations of profiles in a turbulent boundary layer, relative to the location of the interfacial layer, of the conditional mean vorticity and mean velocity.

(a) (b)

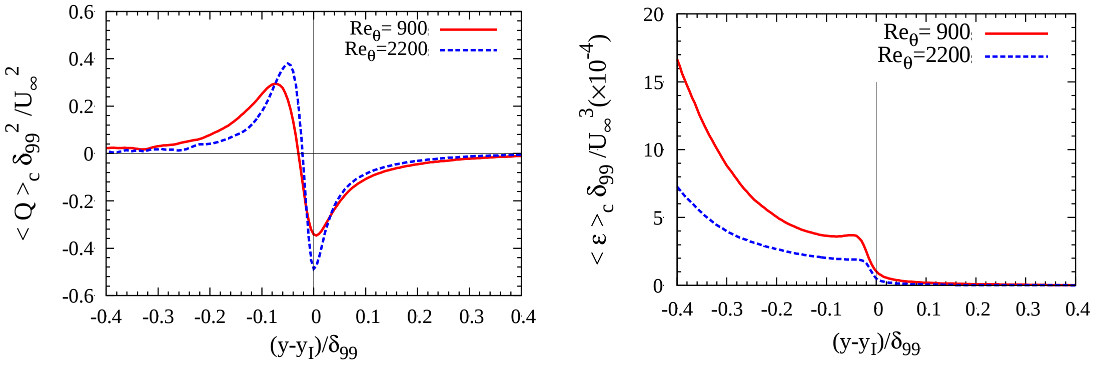

Fig. 3. DNS of the profile of the changing structure of the gradients of velocity fluctuations relative to the interface position of a turbulent boundary layer. (a) Showing rotational strain where the layer adjoins the turbulence, and irrotational strain fluctuations at the edge and outside the layer. (b) Dissipation rate, normalized, showing the sharp gradient at the interfacial layer.

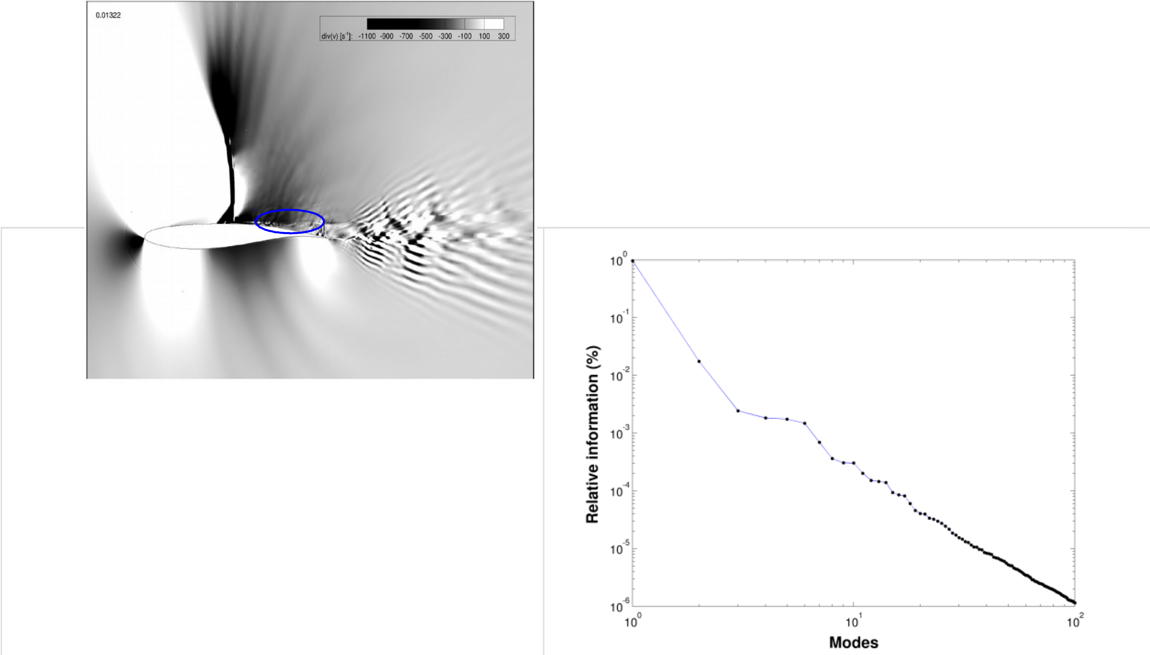

Fig.4. Computation of the transonic interaction over a supercritical airfoil (the OAT15A) by means of the Organised Eddy Simulation, OES. Left: iso-div(**U**) contours showing the wake and the production of waves outside it
Right:

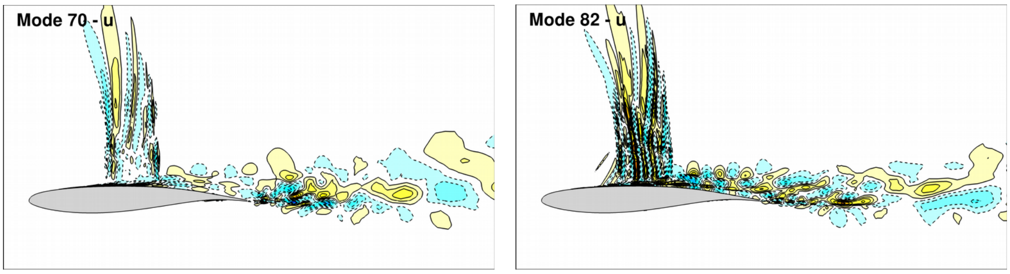

Fig.4b Higher-order POD modes from the OES simulation (Fig. 4a)

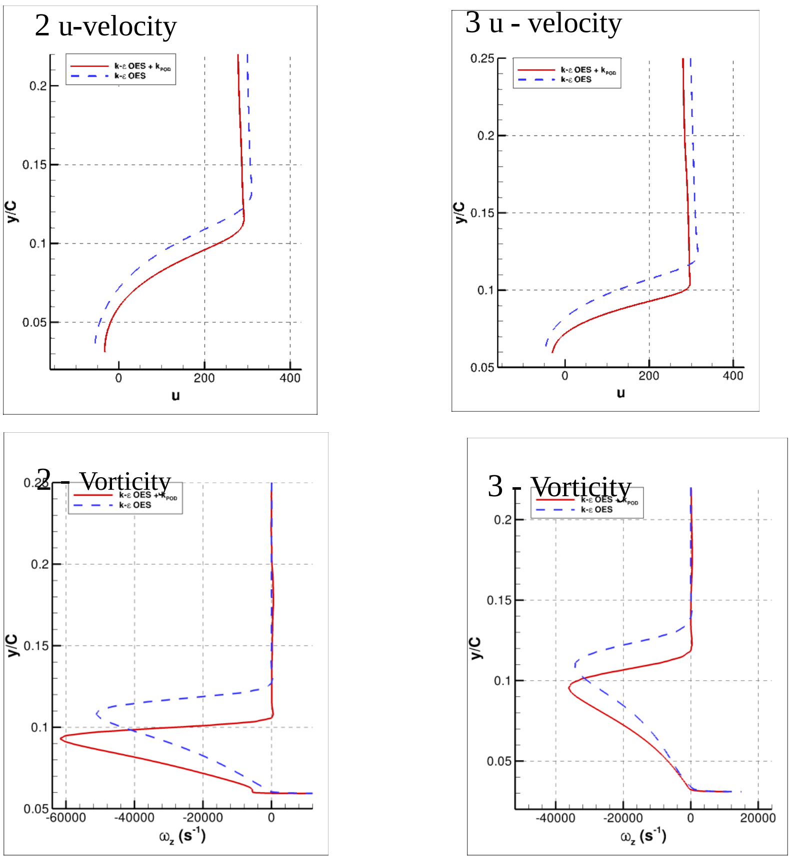

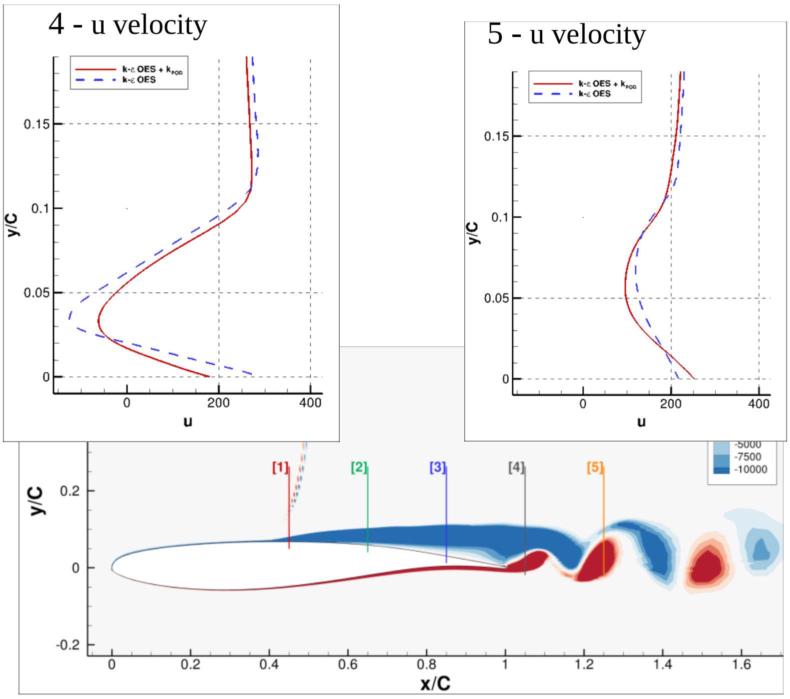

Fig.4c Effect of the stochastic forcing on the velocity and vorticity profiles. The positions are shown in the above figure.
Mean velocity profiles by simulations using the stochastic forcing - IOES (red line) and comparison without forcing - OES (blue line).

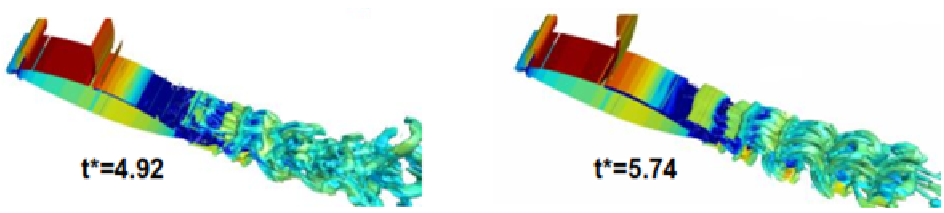

Fig. 5. Illustration of the three-dimensional *Q* criterion coloured by vorticity for two instants corresponding to the upstream and downstream shock motion and to the buffet phenomenon around the V2C supercritical wing at incidence of 7°, free-stream Mach number 0.70 and Reynolds number 3.245×10^6.

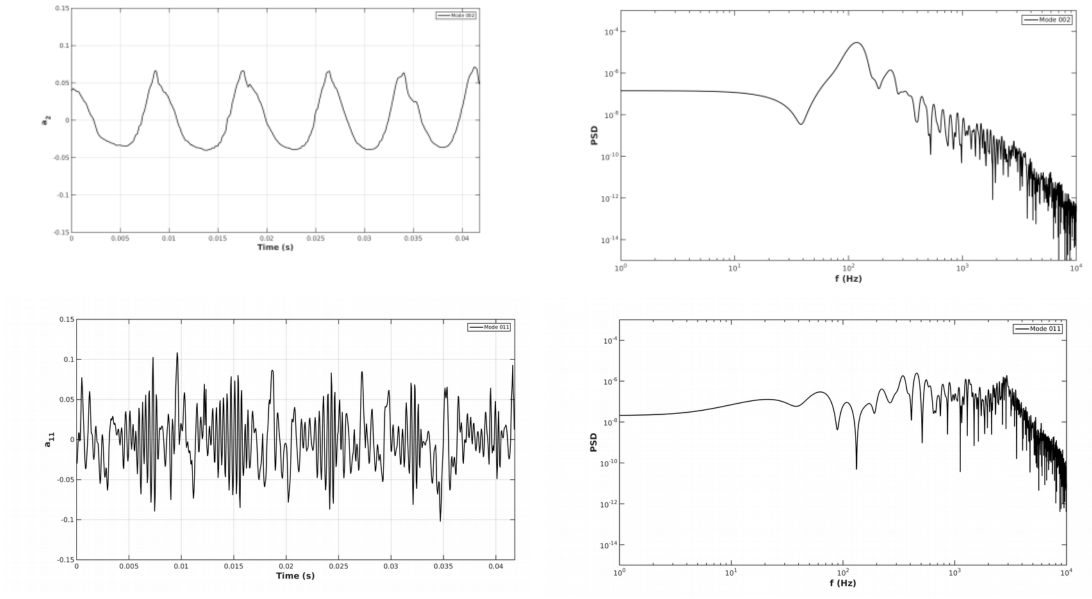

Fig.6. Temporal coefficient of the 2nd-order POD mode (top left) ; spectrum of the 2nd order mode temporal coefficient (top right) illustrating the buffet predominant frequency bump; 11-th order POD mode temporal coefficient (bottom left) and corresponding spectrum (bottom right), illustrating the von Kármán frequency bump (see Fig.5).

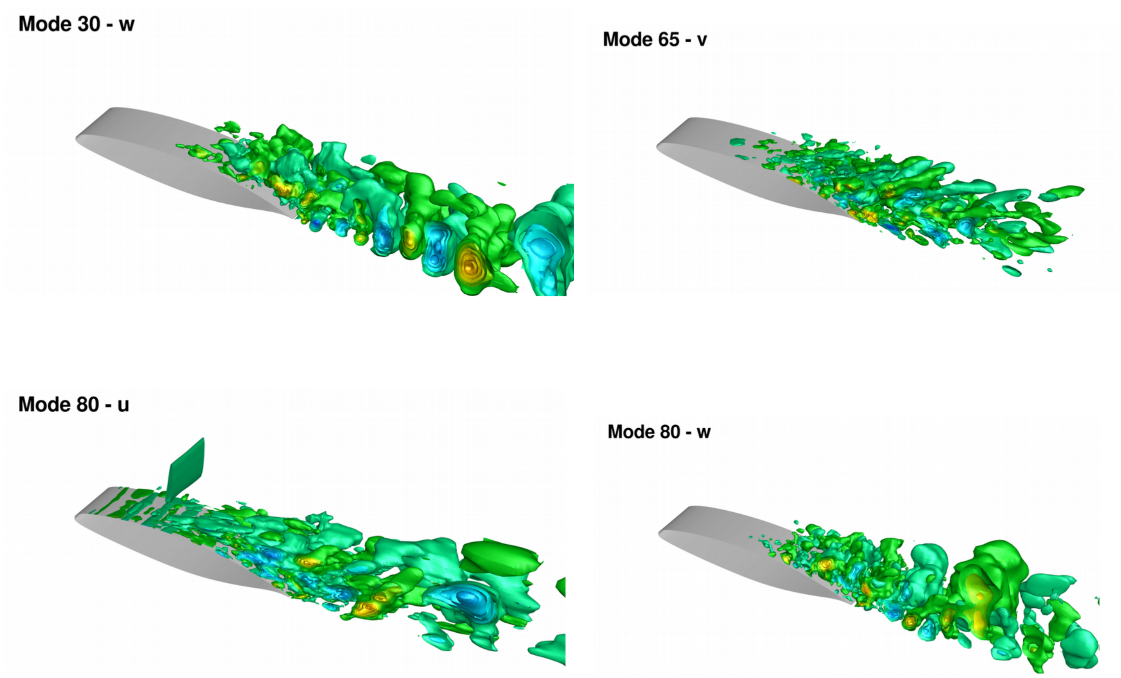

Fig.7. Higher-order POD modes - V2C wing